

Received: 2015.10.31
Accepted: 2015.12.21
Published: 2016.06.16

Value of Three-Dimensional Maximum Intensity Projection Display to Assist in Magnetic Resonance Imaging (MRI)-Based Grading in a Mouse Model of Subarachnoid Hemorrhage

Authors' Contribution:
Study Design A
Data Collection B
Statistical Analysis C
Data Interpretation D
Manuscript Preparation E
Literature Search F
Funds Collection G

CDEF 1 **Tomoko Mutoh***
ABCDEF 1,2 **Tatsushi Mutoh***
ADE 2,3 **Kazumasu Sasaki**
BD 1,4 **Kazuhiro Nakamura**
E 1 **Yasuyuki Taki**
ADEG 2 **Tatsuya Ishikawa**

1 Department of Nuclear Medicine and Radiology, Institute of Development, Aging and Cancer (IDAC), Tohoku University, Sendai, Japan
2 Department of Surgical Neurology, Research Institute for Brain and Blood Vessels-AKITA, Akita, Japan
3 Department of Preclinical Evaluation, IDAC, Tohoku University, Sendai, Japan
4 Department of Radiology, Research Institute for Brain and Blood Vessels-AKITA, Akita, Japan

* Co-first author

Corresponding Author: Tatsushi Mutoh, e-mail: tmutoh@tiara.ocn.ne.jp

Source of support: This work was supported by a Grant-in-Aid for Scientific Research from the Japan Society for the Promotion of Science (15K10966), Life Science Foundation of Japan, and an Institutional Research Grant from Akita Prefecture

Background: Subarachnoid hemorrhage (SAH) is one of the most devastating cerebrovascular disorders. We report on the diagnostic value of three-dimensional (3-D) maximum intensity projection (MIP) reconstruction of T2*-weighted magnetic resonance images (MRI), processed using graphical user interface-based software, to aid in the accurate grading of endovascular-perforation-induced SAH in a mouse model.





Material/Methods: A total of 30 mice were subjected to SAH by endovascular perforation; three (10%) were scored as grade 0, six (20%) as grade 1, six (20%) as grade 2, eight (27%) as grade 3, and seven (23%) as grade 4 according to T2*-weighted coronal slices. In comparison, none of mice were scored as grade 0, eight (27%) as grade 1, five (17%) as grade 2, nine (30%) as grade 3, and eight (27%) as grade 4 based on subsequent evaluation using reconstructed 3-D MIP images.

Results: Mice scored as grade 0 (10%; no visible SAH) on T2*-coronal images were categorized as grades 1 (thin/localized SAH) and 3 (thick/diffuse SAH) according to 3-D MIP images. Grades based on T2* 3-D MIP images were more closely correlated with conventional SAH score ($r^2=0.59$; $P<0.0001$) and neurological score ($r^2=0.25$; $P=0.005$) than those based on T2*-coronal slices ($r^2=0.46$; $P<0.0001$ for conventional score and $r^2=0.15$; $P=0.035$ for neurological score).

Conclusions: These results suggest that 3-D MIP images generated from T2*-weighted MRI data may be useful for the simple and precise grading of SAH severity in mice to overcome the weakness of the current MRI-based SAH grading system.

MeSH Keywords: **Image Processing, Computer-Assisted • Magnetic Resonance Imaging • Mice, C57BL/6 • Subarachnoid Hemorrhage**

Full-text PDF: <http://www.medscimonit.com/abstract/index/idArt/896499>

 1782  —  3  20



Background

Aneurysmal subarachnoid hemorrhage (SAH) is one of the most striking and devastating stroke subtypes in humans [1,2]. In addition to clinical trials aimed at improving outcomes after SAH [3–5], extensive laboratory studies have investigated the pathophysiological mechanisms using rodent models. Experimental SAH is usually established by endovascular perforation, in which an artery of the circle of Willis is perforated using an intraluminal filament [6]. Although this method is considered to provide the best physiological imitation of SAH after aneurysmal rupture in humans, there are currently no useful grading systems for categorizing the severity of SAH in experimental animals on the basis of subarachnoid blood in an *in vivo* setting. Most studies using the endovascular perforation model in rodents confirmed the severity of SAH anatomically by post-mortem exploration of the subarachnoid clot in the extracted brain [7–9], and/or functionally by neurological examination [6, 10, 11].

A more practical grading system based on magnetic resonance imaging (MRI) has recently been proposed in a mouse model of SAH, using T2* gradient-echo (GRE) imaging, without the need for animal euthanasia [12]. Clinically, T2*-weighted sequences are used to depict paramagnetic deoxyhemoglobin, methemoglobin, or hemosiderin in small lesions and tissues [13]. Pathologic conditions that can be visualized by hypointense signals with these sequences include acute SAH and susceptibility vessel sign in acute stroke [13, 14]. Although MRI grading based on T2*-weighted imaging correlates with conventional SAH grading in rodents in terms of severity and neurological score, there remain some difficulties in identifying the SAH clot in two-dimensional (2-D) slices in brain MRI.

In the present study, we introduced a method using three-dimensional (3-D) maximum intensity projection (MIP) reconstruction of T2*-weighted magnetic resonance (MR) images, processed using graphical user interface (GUI)-based software, to aid in the accurate grading of SAH severity in a mouse model. The MIP tool enables manipulation of 3-D renderings of the imaging data, thus allowing easy detection of SAH in mice.

Material and Methods

All experimental protocols in this study were reviewed and approved by the Institutional Animal Care and Use Committee in accordance with the Guidelines for Animal Experimentation at the Research Institute for Brain and Blood Vessels-AKITA. Male C57BL/6N mice weighing 21–26 g purchased from Charles River Laboratories Japan (Kanagawa, Japan) were housed in groups of 5 animals per cage (28×42×20 cm). Mice were maintained at 24±1°C in an air-conditioned environment with a

12-h light/dark cycle and received a standard rodent diet and water *ad libitum*.

A total of 37 mice were used at 9 weeks of age. Microsurgery to induce SAH was performed in 9-week-old mice using aseptic procedures, as described previously [6]. Briefly, mice were premedicated with butorphanol (5 mg/kg, subcutaneous) and anesthetized with isoflurane (2% induction in 2.0 L/min; 1.5% maintenance in 1.0 L/min of 50% O₂ in air) via a facemask. MRI-compatible, non-invasive tail-cuff plethysmography blood pressure, heart rate, arterial oxygen saturation, and rectal temperature sensors were attached in the supine position. Each mouse was placed on a servo-controlled heating blanket and body temperature was monitored via a rectal temperature probe and maintained at 36±1°C. The anesthetic concentrations of isoflurane were titrated within the range of 1.1–1.9%. A 5-0 (0.1-mm diameter) blunted nylon monofilament suture was used for vessel perforation. A midline incision was made in the neck to expose the carotid bifurcation, and then as long a segment of the external carotid artery (ECA) as possible was isolated. The ECA was ligated, coagulated, and cut and a mini clip was placed at the proximal part of the ECA. A small arteriotomy was performed on the distal part of the ECA stump using a 27-G needle tip, and the filament was gently pushed 10–13 mm forward until resistance was felt at the bifurcation of the terminal internal carotid artery and proximal portion of the middle cerebral artery, followed by a further 1–2 mm advancement to perforate the vessel. After achieving hemostasis from the vessels and surrounding tissue, the skin was closed with a 6-0 blue polypropylene monofilament suture. Mice were administered warm, sterile isotonic fluids subcutaneously at 3–5% of body weight prior to and at the end of surgery. The body weights of each animal were recorded daily, and mice without normal daily water consumption within 24 h of recovery from anesthesia received a 1.5–2 mL of warm 5% w/v dextrose solution subcutaneously.

All MR data were acquired under isoflurane anesthesia within 24 h after SAH induction, using a 4.7 Tesla Varian MRI scanner (Varian Inc., Palo Alto, CA, USA) equipped with a 12-cm internal diameter gradient coil and a 72-mm internal diameter cylindrical probehead. Whole-brain MRI was performed to ensure correct head positioning with acquisition of T2* GRE sequences (long repetition time/short echo time/flip angle=20 ms/10 ms/20°) with a field of view of 20×20×20 mm, matrix size of 128×128×128 mm, and 25 coronal slices (0.5-mm thick), as described previously [12]. An MIP was then generated from a 3-D reconstruction of the T2*-weighted slices using a free GUI-based analysis tool to support DICOM image conversion into NIfTI format (MRICron [15]).

We categorized the mice into five grades according to the thickness of the SAH clot and the presence of intraventricular

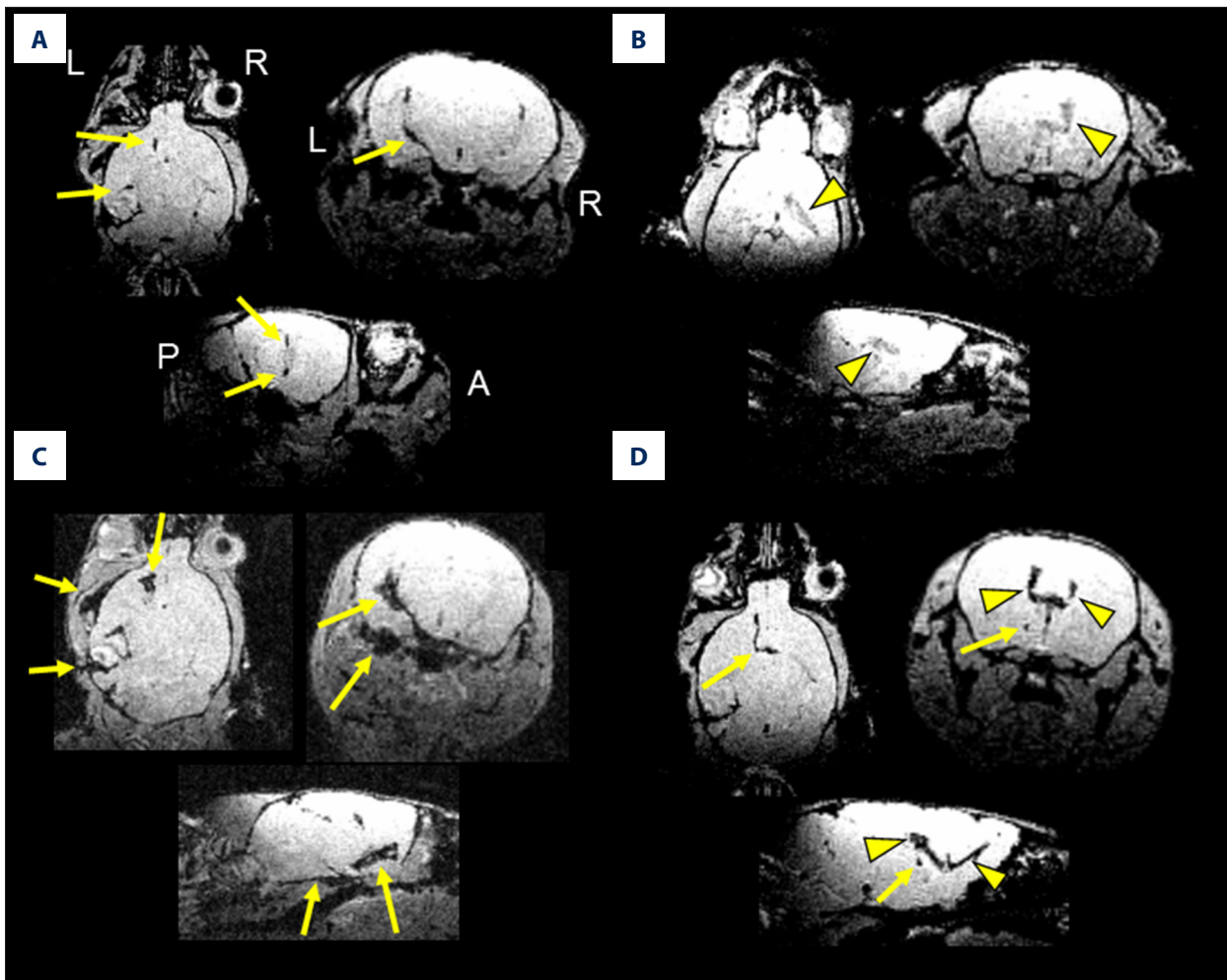


Figure 1. Examples of SAH grades based on 3-D MIP images reconstructed from T2*-weighted MRI slices in mice. Grade 1 (minimal/localized SAH with no IVH) (A); grade 2 (minimal/localized SAH with IVH) (B); grade 3 (thick/diffuse SAH with no IVH) (C); and grade 4 (thick/diffuse SAH with IVH) (D). Upper left, upper right, and lower images in each panel show axial, coronal, and sagittal sections, respectively. Arrows indicate superficial and/or basal SAH clot, and arrowheads indicate IVH. L – left; R – right; A – anterior; P – posterior.

hemorrhage (IVH) [12] detected by coronal slices and by reconstructed 3-D MIP images of T2*-weighted sequence. Grade 0=no visible SAH or IVH; grade 1=minimal/localized SAH with no IVH; grade 2=minimal/localized SAH with IVH; grade 3=thick/diffuse SAH (hematoma >0.5 mm thick visible in >2 slices of T2*-weighted images) with no IVH; and grade 4=thick/diffuse SAH with IVH. Image interpretation was initially performed with T2*-weighted coronal slices for the initial score, followed by 3-D MIP display for the final score. After completion of data acquisition, the SAH grades were examined by two investigators (KS and KN) to avoid bias and to examine the reproducibility of the grading system, and the final decision for data analysis was made by TM.

Neurological scores of 3–18 in single-increment steps (higher scores indicate greater function) were evaluated at 24 h after SAH by a single, blinded observer (TM), as described

previously [11]. After completion of the experiment, mice were euthanized by an overdose of pentobarbital (200 mg/kg, intraperitoneal) and the brains were examined to assess the severity of SAH using a conventional grading system [10]. The animals were assigned a total score ranging from 0 to 18 by summing the scores from all six segments in the basal brain.

Statistical analysis was carried out using SigmaPlot version 13 (Systat Software Inc., CA, USA). Correlations between MRI grade and conventional SAH severity score based on the evaluation of blood clots and neurological score were examined by Spearman's rank correlation tests. Non-parametric data were compared using the Kruskal-Wallis test. The Cohen κ (K_c) and weighted κ (K_w) values were calculated to examine reproducibility of the scale between the two investigators [16]. Values of $P < 0.05$ were considered statistically significant.

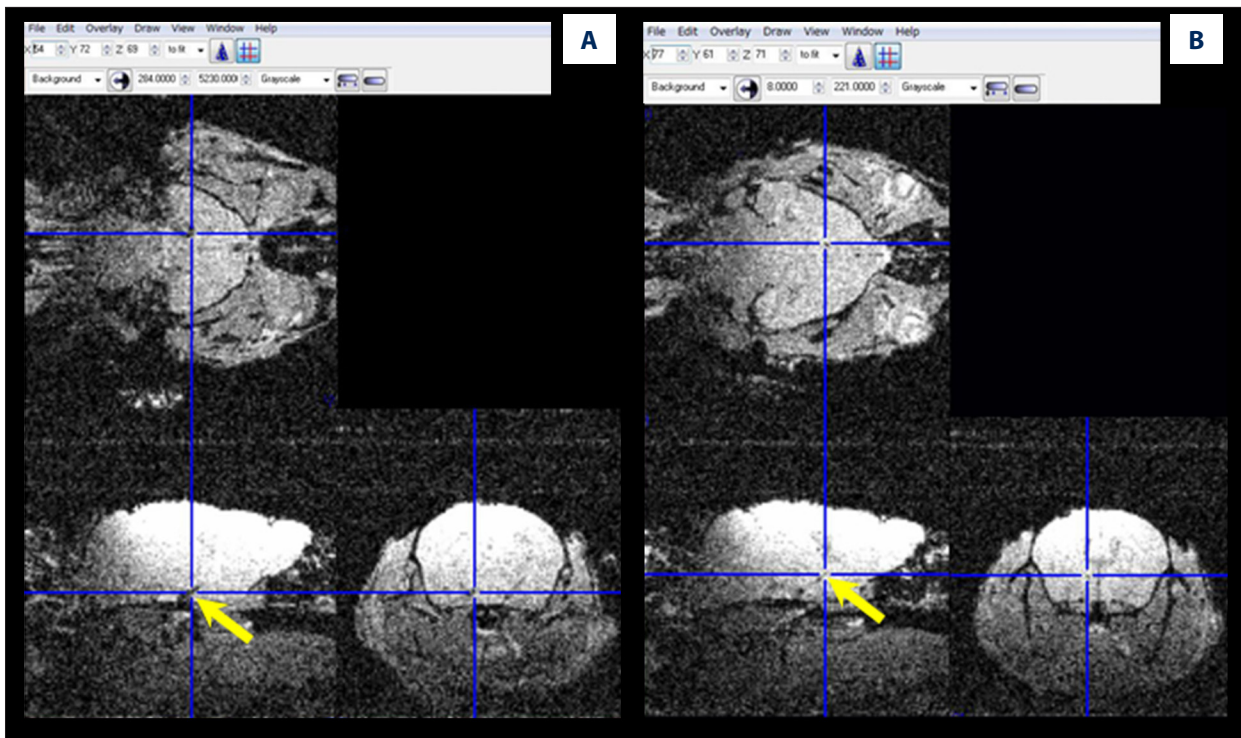


Figure 2. Examples of a mouse SAH model in which the MRI-based diagnoses changed from grade 0 to 1 (A) and grade 2 to 4 (B) after interpretation of 3-D MIP images reconstructed from T2*-weighted MRI slices. Arrows indicate superficial and/or basal SAH clot.

Results

The mortality in this study was 19% (7/37) at 24 h after SAH induction, which is in agreement with previously published data [7,9,12,17]. Among the total of 30 mice, three (10%) were scored as grade 0, six (20%) as grade 1, six (20%) as grade 2, eight (27%) as grade 3, and seven (23%) as grade 4 for initial evaluation using T2*-coronal slices. In contrast, eight (27%) were scored as grade 1, five (17%) as grade 2, nine (30%) as grade 3, and eight (27%) as grade 4 on final evaluation, assisted by 3-D MIP images. Representative 3-D MIP images for SAH grades 1–4 are shown in Figure 1A–1D, respectively. Assisted by axial and sagittal T2*-weighted MIP images, SAH was predominantly observed in the left cortical surface by sagittal section and the basal cistern by axial section (Figure 1A, 1C), where the terminal internal carotid artery was perforated. However, IVH localized in the third and lateral ventricles was visualized mainly by coronal slices (Figure 1B, 1D). Examples of SAH-induced mice in which the diagnoses changed from grade 0 to 1 and grade 2 to 4 after interpretation of 3-D MIP images are shown in Figure 2A, 2B, respectively. In these cases, basal and superficial SAH clots were more effectively visualized by para-sagittal plane images as compared to the images within a single coronal slice.

There were significant correlations between MRI grade and conventional SAH score ($r^2=0.46$; $P<0.0001$ for initial evaluation (Figure 3A) and $r^2=0.59$; $P<0.0001$ for final evaluation (Figure 3B)) and between MRI grade and neurological score ($r^2=0.15$; $P=0.035$ for initial evaluation (Figure 3C) and $r^2=0.25$; $P=0.005$ for final evaluation (Figure 3D)), with 3-D MIP-based MRI interpretation demonstrating a stronger relationship. With regard to interobserver variability, the Kw value for the thickness of the subarachnoid clot and Kc value for the presence of IVH in the lateral ventricle were 0.89 and 0.81, respectively (for initial score) and 0.95 and 0.90, respectively (for final score). Kw value for the MRI grading scale was 0.94. The system was therefore considered to have excellent reproducibility.

Discussion

An MIP is a series of 2-D images generated from a 3-D rendering of MRI data by selecting the maximum value through the reconstruction seen by each 2-D pixel at each of several viewing angles. Each angular view in an MIP thus has a unique viewing angle that defines the 2-D projection plane. This technique is useful for detecting small lesions in the lungs and mammary glands in clinical practice. Interestingly, the proportion of mice in the current study scored as grade 0 was reduced using 3-D MIP, and they were assigned mainly to grades 1 and 3 on final

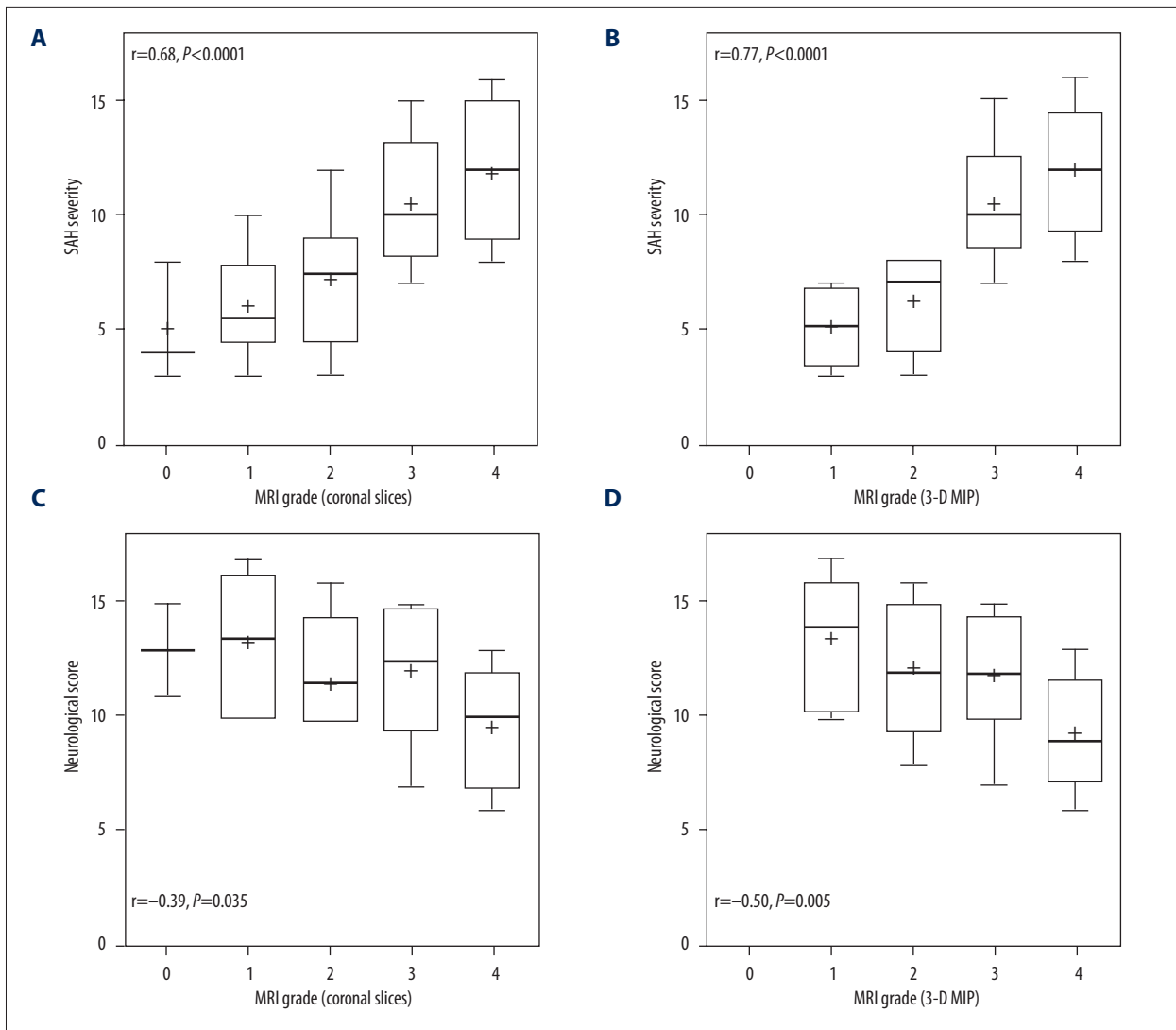


Figure 3. Relationships between MRI grading (0–4) and conventional SAH score and neurological score on initial evaluation with T2*-weighted coronal slices (**A, C**) and final evaluation with reconstructed 3-D MIP images (**B, D**). (+) in each bar indicates mean value.

evaluation, suggesting that this method increased the precision in relation to the severity and localization of the SAH clot.

The MRI-based grading scale imitates the human SAH scale using a computed tomography scan (e.g., modified Fisher scale) [18]. Our results suggest that additional 3-D MIP studies exploring SAH and IVH may strengthen the relationships of this grading system with both conventional SAH grade and functional outcome scores compared with single evaluation using T2*-weighted coronal slices alone. The easy-to-use software used in the present study allows the integration of T2*-weighted slice data into one image to provide more accurate SAH grading. Although we used T2*-weighted images to examine the severity and location of SAH based on recent results [12, 19], sequences such as fluid-attenuated inversion

recovery (FLAIR) and susceptibility-weighted images [20] warrant further investigation.

Conclusions

Our results provide the first evidence demonstrating the feasibility of 3-D MIP images generated from GUI-based software for the simple and precise SAH grading in a mouse model of endovascular perforation technique to overcome the weakness of the current MRI-based SAH grading system.

Conflicts of interest statement

The authors declare that they have no competing interests.

References:

1. Juszkat R, Jonczyk-Potoczna K, Stanislawska K et al: Endovascular treatment of an adolescent patient with a ruptured intracranial aneurysm – case report and review of literature. *Pol J Radiol*, 2015; 80: 10–12
2. D'Souza S: Aneurysmal subarachnoid hemorrhage. *J Neurosurg Anesthesiol*, 2015; 27: 222–40
3. Mutoh T, Kazumata K, Terasaka S et al: Early intensive versus minimally invasive approach to postoperative hemodynamic management after subarachnoid hemorrhage. *Stroke*, 2014; 45: 1280–84
4. Mutoh T, Kazumata K, Ishikawa T et al: Performance of bedside transpulmonary thermodilution monitoring for goal-directed hemodynamic management after subarachnoid hemorrhage. *Stroke*, 2009; 40: 2368–74
5. Macdonald RL: Delayed neurological deterioration after subarachnoid haemorrhage. *Nat Rev Neurol*, 2014; 10: 44–58
6. Buhler D, Schuller K, Plesnila N: Protocol for the induction of subarachnoid hemorrhage in mice by perforation of the circle of willis with an endovascular filament. *Transl Stroke Res*, 2014; 5: 653–59
7. Schuller K, Buhler D, Plesnila N: A murine model of subarachnoid hemorrhage. *J Vis Exp*, 2013; 81: e50845
8. Muroi C, Fujioka M, Okuchi K et al: Filament perforation model for mouse subarachnoid hemorrhage: Surgical-technical considerations. *Br J Neurosurg*, 2014; 28: 722–32
9. Friedrich B, Muller F, Feiler S et al: Experimental subarachnoid hemorrhage causes early and long-lasting microarterial constriction and microthrombosis: An *in-vivo* microscopy study. *J Cereb Blood Flow Metab*, 2012; 32: 447–55
10. Sugawara T, Ayer R, Jadhav V et al: A new grading system evaluating bleeding scale in filament perforation subarachnoid hemorrhage rat model. *J Neurosci Methods*, 2008; 167: 327–34
11. Altay O, Hasegawa Y, Sherchan P et al: Isoflurane delays the development of early brain injury after subarachnoid hemorrhage through sphingosine-related pathway activation in mice. *Crit Care Med*, 2012; 40: 1908–13
12. Egashira Y, Shishido H, Hua Y et al: New grading system based on magnetic resonance imaging in a mouse model of subarachnoid hemorrhage. *Stroke*, 2015; 46: 582–84
13. Chavhan GB, Babyn PS, Thomas B et al: Principles, techniques, and applications of T2*-based mr imaging and its special applications. *Radiographics*, 2009; 29: 1433–49
14. Kimura K, Iguchi Y, Shibazaki K et al: M1 susceptibility vessel sign on t2* as a strong predictor for no early recanalization after iv-t-pa in acute ischemic stroke. *Stroke*, 2009; 40: 3130–32
15. Rorden C, Karnath HO, Bonilha L: Improving lesion-symptom mapping. *J Cogn Neurosci*, 2007; 19: 1081–88
16. Kundel HL, Polansky M: Measurement of observer agreement. *Radiology*, 2003; 228: 303–8
17. Plesnila N: Pathophysiological role of global cerebral ischemia following subarachnoid hemorrhage: The current experimental evidence. *Stroke Res Treat*, 2013; 2013: 651958
18. Claassen J, Bernardini GL, Kreiter K et al: Effect of cisternal and ventricular blood on risk of delayed cerebral ischemia after subarachnoid hemorrhage: The fisher scale revisited. *Stroke*, 2001; 32: 2012–20
19. Shishido H, Egashira Y, Okubo S et al: A magnetic resonance imaging grading system for subarachnoid hemorrhage severity in a rat model. *J Neurosci Methods*, 2015; 243: 115–19
20. Verma RK, Kottke R, Andereggen L et al: Detecting subarachnoid hemorrhage: Comparison of combined FLAIR/SWI versus CT. *Eur J Radiol*, 2013; 82: 1539–45